Proceedings 10th NUMGE 2023
10th European Conference on Numerical Methods in Geotechnical Engineering
Zdravkovic L, Kontoe S, Taborda DMG, Tsiampousi A (eds)

https://doi.org/10.53243/NUMGE2023-284

Investigation of a hypoplastic model with two different intergranular strain extensions for undrained behaviour of silty sand

A.O. Abdelkadr[1], O. Reul[1], T. Wichtmann[2]

[1]*Department of Geotechnical Engineering, University of Kassel, Kassel, Germany*
[2]*Chair of Soil Mechanics, Foundation Engineering and Environmental Geotechnics, Ruhr University, Germany*

ABSTRACT: This paper describes the results of a back analysis of element tests with monotonic and cyclic loading on a silty sand applying a hypoplastic constitutive model together with two different intergranular strain extensions. The material used in the experiments is an Ethiopian sand with 35.5% non-plastic fines content. After calibration of the material parameters, element test simulations were performed. In a first step, the performance of the constitutive model was studied by comparing the calculated and measured stress-strain relationships and effective stress paths from undrained monotonic triaxial tests with different initial pressures. In a second step, a comparison of numerical and experimental data was undertaken for undrained cyclic triaxial tests performed with different cyclic stress ratios CSR [0.25 to 0.75] and relative densities D_r [20% to 50%]. In the latter case, the comparison focussed on the build-up of excess pore water pressure and the accumulation of axial strain with increasing number of cycles. The results showed the capability of the hypoplastic constitutive model and its extensions to simulate the cyclic behaviour and the liquefaction potential of the silty sand, but also revealed limitations in some cases.

Keywords: silty sand; liquefaction; hypoplasticity; intergranular strain extension; coupled pore pressure-displacement analysis

1 INTRODUCTION

During static or cyclic loadings, water-saturated granular soils with loose to medium dense packing tend to achieve a denser configuration (Lade and Yamamuro 1999). However, due to the limited duration to dissipate excessive pore water in case of rapid loading (e.g. earthquakes), a build-up of excess pore water pressure instead of densification occurs under undrained conditions. With increasing pore water pressure, the effective stress reduces resulting in significant loss of shear strength and/or excessive deformation.

The liquefaction of sands has been investigated since the 1960s following the Alaska and Niigata earthquakes (Ertek and Demir 2017). In the last decade, particularly following the extensive liquefaction events during the earthquake in Christchurch 2011, the cyclic behaviour and liquefaction resistance of silty sands has increasingly attracted attention. Researchers (e.g. Belkhatir et al. (2010)) have presented valuable experimental results concerning the cyclic behaviour and liquefaction phenomena of clean sands and sand-fine mixtures. Most of these studies have demonstrated that silty sands can liquefy easier than clean sands.

Furthermore, an evaluation of the cyclic behaviour and liquefaction risk of soil deposits or geotechnical structures using numerical methods is being applied more frequently. In this regard, significant progress has been made in the last decades with respect to the simulation of stress-strain behaviour, pore pressure build-up and liquefaction potential of granular soils under cyclic loading as summarised e.g. by Abdelkadr (2023).

Several studies on liquefaction analyses documented in the literature have used constitutive models based on multi-surface and bounding plasticity, critical-state theory or hypoplasticity. Bao and Sture (2011) used a kinematic-cyclic constitutive model based on fuzzy-set concepts and incremental plasticity theory for modelling the cyclic mobility of saturated granular soil. Examples for the applications of hypoplastic constitutive models in the liquefaction analysis can be found in the works of e.g. Cudmani (2013) and Hleibieh and Herle (2019). These studies show that the evaluation of liquefaction based on numerical simulations requires rather advanced constitutive models to realistically represent the soil behaviour considering continuously changing soil properties under cyclic loading.

In the scope of this paper, the results of a numerical investigation on cyclic behaviour and liquefaction potential applying a hypoplastic soil model and its extensions for silty sand sampled from seismically active sites in Ethiopia are presented.

2 SOIL SAMPLE AND PROPERTIES

In the current study, two phases of assessments were performed. First, four soil samples were collected at a depth of 3 m below ground level from four seismically

active sites, close to the city of Mekelle, Ethiopia, where on April 24, 2018, an earthquake having a local magnitude M_L = 5.2 was recorded (USGS 2019). Mekelle is located in the Main Ethiopian Rift (MER) which is connected to the well-known East Africa Rift System (EARS) that is described as extensional active tectonics (Bonini et al. 2005).

During the first phase, preliminary screening using the composition criterion was used to select a likely liquefiable soil sample for further investigations (second phase). Details on analyses and procedures can be found in Abdelkadr (2023). Figure 1 shows the gradation test results for sample TP-1 drawn together with the definition of potentially liquefiable and most liquefiable boundary curves proposed by Tsuchida (1970). Hence, sample TP-1, which contains 65.5% sand, 28.3% silt, and 6.2% clay by mass, was used for this study in the second phase. Table 1 presents a summary of the index properties of sample TP-1.

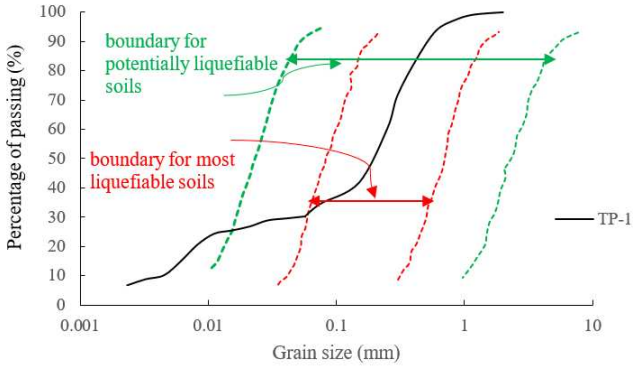

Figure 1. Gradation curves and boundaries for liquefiable and non-liquefiable soils redrawn after Tsuchida (1970).

Table 1. Summary of index properties of sample TP-1

Index Property	Symbol	Unit	Value
Specific gravity	G_s	-	2.66
Sand content	-	%	65.5
Silt content	-	%	28.3
Clay content	-	%	6.2
Maximum void ratio	e_{max}	-	1.093
Minimum void ratio	e_{min}	-	0.491
Effective size diameter	d_{10}	mm	0.005
Average size diameter	d_{50}	mm	0.194
Uniformity coefficient	C_u	-	41.7
Curvature coefficient	C_c	-	2.4

In the second phase the behaviour of the silty sand sample TP-1 during undrained monotonic and cyclic loading was investigated for different initial densities and confining pressures using triaxial tests (Abdelkadr et al. (2022), Abdelkadr (2023)). All tests were completed on isotropically consolidated specimens. Besides, oedometric tests with incremental loading were also performed considering different initial densities.

In general, the tests were used not only to evaluate the liquefaction potential but also to calibrate the parameters of material models used in numerical analyses to study soil behaviour as documented by Abdelkadr (2023). The present paper focusses on one part of the numerical study, namely the evaluation of the performance of the applied hypoplastic model and its extensions in element test simulations and the comparison with the experimental results.

3 NUMERICAL MODEL

3.1 General remarks

The simulations of the element tests were performed under similar initial states and loading conditions as the experiments. The simulations were carried out for tests which were not used during the initial calibration of the model parameters. In this study, the hypoplastic model by von Wolffersdorff (1996) with its intergranular strain extensions was applied as the constitutive model.

All numerical simulations presented in this paper have been carried out with the FE code Tochnog (Tochnog Professional Company 2021) applying a single quadrilateral element with both displacements and pore pressures varying linearly across the element in a coupled pore pressure - displacement analysis.

3.2 Constitutive model

3.2.1 The hypoplastic (HP) model

The hypoplastic model is an incrementally non-linear constitutive model and, unlike in elasto-plastic models, the strain rate is not decomposed into elastic and plastic parts, and nor does it require the yield and plastic potential surfaces. Various versions of the hypoplastic model have been developed but the important step forward was the implementation of the critical state concept and inclusions of the influence of the stress level (barotropy) and the influence of density (pyknotropy). Nowadays, the model in the version proposed by von Wolffersdorff (1996), who incorporated the Matsuoka-Nakai surface for critical state stress conditions, can be considered as a standard hypoplastic (HP) model for granular materials (Herle and Gudehus 1999). The HP model is capable of predicting important features of the soil behaviour, such as the critical state, dependency of the peak strength on soil density, non-linear behaviour for a range of strains and dependency of the soil stiffness on the loading direction.

Generally, the von Wolffersdorff (1996) HP model requires eight parameters: φ_c is the critical state friction angle; the granular stiffness h_s and the exponent n control the shape of the limiting void ratio vs. mean effective stress curves (normal compression and critical state lines); e_{d0}, e_{c0}, and e_{i0} are reference void ratios specifying the limiting void ratios corresponding to the densest,

critical and loosest state at zero pressure, respectively; exponent α controls the dependency of peak friction angle φ_p on relative density while the exponent β controls the dependency of stiffness on relative density.

The HP model for granular materials performs reasonably well under monotonic loading. However, its application to cyclic stresses or deformation with small amplitude reveals some limitations (Niemunis and Herle 1997). It specifically leads to excessive accumulation of deformations for small stress cycles, an effect known as ratcheting as shown in Figure 2. Analogously, under small strain cycles the relaxation is predicted by far too fast (Figure 2a). Also, in undrained cyclic shearing, the model predicts a too large build-up of pore pressure. Furthermore, neither the small strain stiffness nor the effects of recent history have been considered in the original model (Niemunis and Herle 1997). Thus, Niemunis and Herle (1997) extended the model to overcome these limitations during stress or strain reversals with the intergranular strain concept.

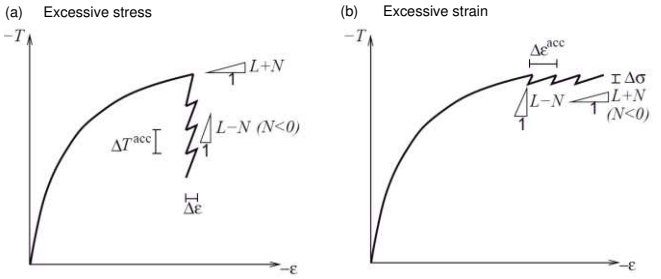

Figure 2. Ratcheting effects after Niemunis and Herle (1997) during a) strain cycles and b) stress cycles

3.2.2 Intergranular strain (IS) extension

Niemunis and Herle (1997) described the deformation of soil as a result of the deformation of the intergranular interface termed as the intergranular strain (δ) and the rearrangement of the soil skeleton. The intergranular strain (IS) extension by Niemunis and Herle (1997) incorporates this intergranular strain in the basic equations of the HP model.

To improve the prediction with respect to the accumulation of volumetric strains under drained conditions or excess pore pressures under undrained conditions, particularly for cyclic loadings with amplitudes of different magnitudes, a further modification to the intergranular strain concept was later incorporated by Wegener and Herle (2014).

The IS extension of Niemunis and Herle (1997) requires five additional parameters, namely the maximum value of intergranular strain R, m_R and m_T which control the initial shear modulus upon 180^0 and 90^0 strain path reversal, respectively, and x and β_r which control the rate of degradation of the stiffness with increasing strain. The further modification of Wegener and Herle (2014) introduces another parameter ϑ which additionally controls the accumulation of permanent deformation and pore water pressures, respectively.

3.2.3 Intergranular strain anisotropy (ISA) extension

Similar to the IS extension, the intergranular strain anisotropy (ISA) extension by Poblete et al. (2016) modifies existing hypoplastic relations to extend their capabilities for cyclic loading. Despite another constitutive formulation the ISA uses four parameters which are similarly applied by the IS approach, namely R, m_R, x and β_r, plus two additional parameters C_a and χ_{max}. The ISA extension enables the simulation of small strain effects, such as the increased stiffness and the reduction of plastic accumulation under repetitive loops.

3.3 Calibration of model parameters

The calibration of the HP parameters mainly followed the approach of Herle and Gudehus (1999). Calibration of the IS and ISA extension parameters is discussed by Niemunis and Herle (1997) and Poblete et al. (2016), respectively, and the parameters were calibrated by means of simulation of cyclic undrained triaxial tests.

Further calibration steps were carried out by means of a parametric study on the influence of the model parameters to achieve a better agreement between the numerical simulations and the test results. Figure 3 shows a typical response for the variation of the parameter R corresponding to the maximum value of intergranular strain for an undrained cyclic test on a specimen with a relative density D_r = 55.3% consolidated to an initial mean effective stress p'_0 = 100 kPa and loaded with a double deviatoric stress amplitude of $2q_{cyc}$ = 50 kPa and a constant frequency of loading, f = 0.5 Hz. It should be mentioned that in the tests of the current study, the cycles were applied with a minimum deviatoric stress q_{min} = 0 and a maximum value q_{max} = 2 q_{cyc}, that means an average deviatoric stress q_{av} = q_{cyc}. The four diagrams in Figure 3 show the development of axial strain ε_a and pore water pressure ratio $r_u = \Delta u/p_0' \cdot 100\%$ with increasing number of cycles N_c, as well as the effective stress path in the q-p' diagram and the stress-strain relationship in the q-ε_a diagram.

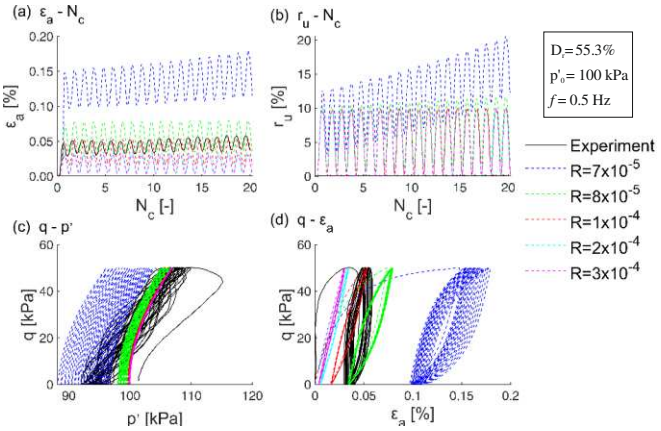

Figure 3. Effect of varying R on predicted undrained cyclic responses and comparison with the experimental data

As typical for tests with an anisotropic average stress, the experimental data in Figure 3 show an accumulation of both axial strain and excess pore water pressure with increasing N_c. Furthermore, the effective stress path does not reach zero effective stress (i.e. p' = 0). Considering the simulations, a lower R value leads to a faster accumulation of axial strain and excess pore water pressure. It may be concluded that with a value of $R = 10^{-4}$ the numerical prediction fits best to the experimental data. In a similar way the other parameters of the IS and ISA extensions were calibrated.

Abdelkadr (2023) gives a detailed description of the calibration process for sample TP-1 resulting into the parameters summarised in Table 2.

Table 2. Material parameters of sample TP-1

HP model parameters					
φ_c	[^{0}]	31.7	e_{c0}	[-]	1.320
h_s	[MPa]	17.9	e_{d0}	[-]	0.491
n	[-]	0.22	e_{i0}	[-]	1.584
α	[-]	0.05	β	[-]	0.80
IS and ISA extension parameters					
R	[-]	$1 \cdot 10^{-4}$	β_r	[-]	0.05
m_R	[-]	4.0	χ	[-]	1
m_T	[-]	2.8	ϑ	[-]	10
Additional parameters for the ISA extension					
C_a	[-]	0.002	χ_{max}	[-]	8

4 COMPARISON OF EXPERIMENTAL DATA AND NUMERICAL SIMULATIONS

4.1 Monotonic test responses

All simulations of the monotonic tests have been performed using the HP model with the IS extension. A comparison of IS and ISA has not been undertaken considering that these extensions are of minor importance for the predicted monotonic behaviour. Initially, all the components of the intergranular strain tensor have been set to zero.

Figure 4 and Figure 5 compare the measured and calculated responses for two specimens with initial conditions of $D_r = 22.7\%$ consolidated to $p'_0 = 50$ kPa and $D_r = 30.8\%$ consolidated to $p'_0 = 200$ kPa, respectively. The four diagrams present the development of deviatoric stress q, stress ratio q/p' and excess pore water pressure Δu with increasing axial strain ε_a, as well as the effective stress path in the q-p' plane.

A reasonable agreement between the experimental and numerical curves can be concluded from both diagrams. The deviation between the simulation responses and the experimental results tends to increase slightly with an increase in the initial effective mean stress. Nevertheless, the measured and calculated responses indicate purely contractive behaviour with a continuous growth of Δu (Figure 4(b) and Figure 5(b)) that leads to a decrease of p' (Figure 4(c) and Figure 5(c)). Similar responses were observed in other tests as well as numerical simulations for different initial conditions (Abdelkadr 2023).

A further comparison between the simulations and experiments is done based on characteristic points during the test, i.e. the peak or instability and steady states. In the experiments the peak states are observed and thus evaluated at relatively small strains. The steady state (SS) corresponds to the state where shearing is continued but neither the deviatoric stress nor the excess pore water pressure or the effective mean stress change anymore. In the current study the steady state is evaluated at an axial strain $\varepsilon_a = 20\%$. The decrease of deviatoric stress after the peak characterises a strain softening behaviour and it indicates an unstable soil state. The line connecting the peak deviatoric stresses in a p'- q plot is referred to as the instability line ISL while at the steady state it is termed the steady state line SSL. The zone bounded by ISL and SSL is the zone of instability (Lade and Yamamuro 1999).

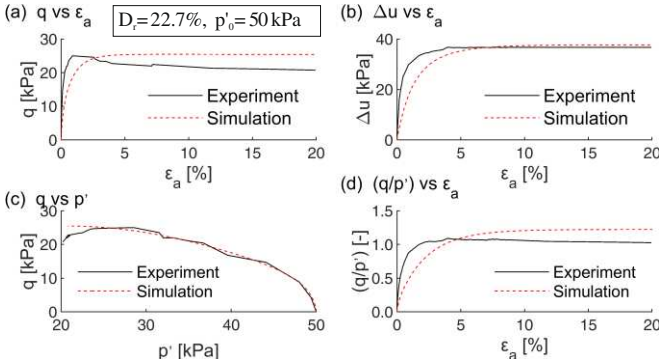

Figure 4. Comparison of undrained monotonic responses

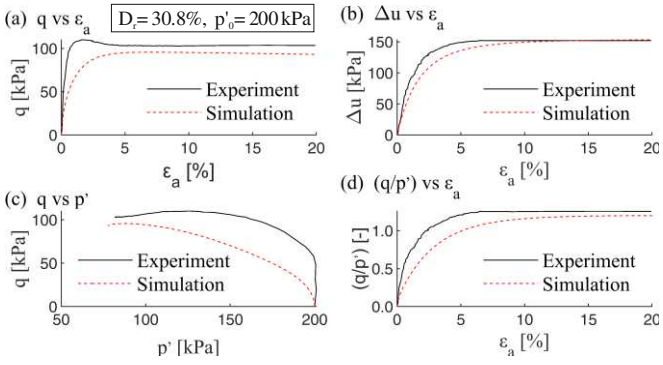

Figure 5. Comparison of undrained monotonic responses

Stresses and excess pore water pressures at peak and steady state are compared in Figure 6 for all monotonic tests. Figure 6(a) and (b) shows the comparison of the

stress states at peak and at the steady state SS, respectively. As can be observed from the plots, the data falls in a relatively narrow band with a slight variation between simulated and measured values. Figure 6 (a) and (b) indicate average slopes of the ISL and SSL. While the predicted ISL lies slightly above the experimental one, it is the other way around in case of the SSL. It can be observed that the responses are somewhat more consistent at SS than that at the peak state.

Figure 6(c) and Figure 6(d) show the comparisons of the excess pore pressures at peak and steady state, respectively. When compared at the same effective mean stress for the peak state conditions the numerically computed pore pressure build-up is higher than in the test results (Figure 6(c)). Nevertheless, the excess pore pressures at the SS are in reasonable agreement with the experimental results (Figure 6(d)).

Based on Figure 4 to Figure 6 it may be concluded that with few exceptions the hypoplastic model of von Wolffersdorff performs well to describe the behaviour of the silty sand under undrained monotonic loading.

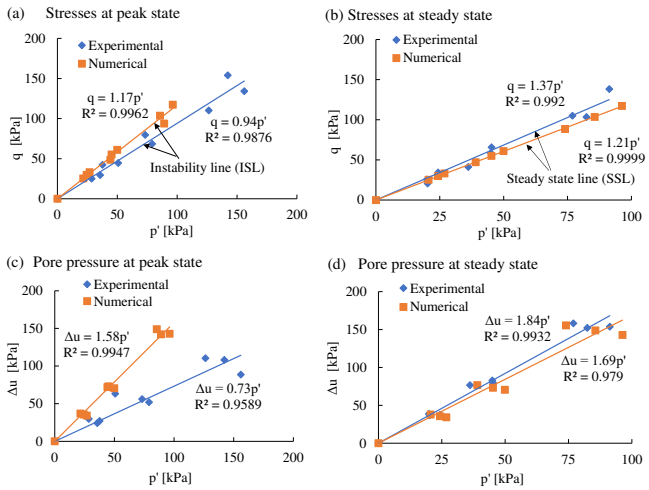

Figure 6. Comparison of peak and steady states for undrained monotonic loading

4.2 Cyclic test responses

The comparison between the experimental data and numerical simulations was carried out for both extensions, the IS and the ISA approach. The comparison is done based on tests which have not been used for the calibration of the model parameters.

Figure 7 compares the response with the IS extension for a specimen tested with the initial conditions of D_r = 51.4% consolidated to p'_0 = 50 kPa. As can be observed from Figure 7(a), the numerical simulation resulted in a strain accumulation which was significantly larger than in the experiment. Moreover, the pore pressure also showed a faster build-up compared to the experimental results (Figure 7(b)) with r_u = 100% reached in two cycles, N_{cl} = 2, while the experiments showed N_{cl} = 5. Similar investigations were carried out on other specimens and showed the same deviation (Abdelkadr 2023).

Figure 8 shows the comparison of the test with a numerical simulation applying the hypoplastic model with the ISA extension. It can be seen that the computed axial strain values were in the same order, but slightly smaller than the experimental results (Figure 8(a)). The predicted course of excess pore water pressure with increasing number of cycles was also in good agreement with the experiment. Hence, the implementation of the ISA extension by means of considering the two additional parameters C_a and χ_{max} has significantly improved the agreement between the experiment and simulation for the accumulation of strains (Figure 8(a)) and the build-up of pore pressure (Figure 8(b)).

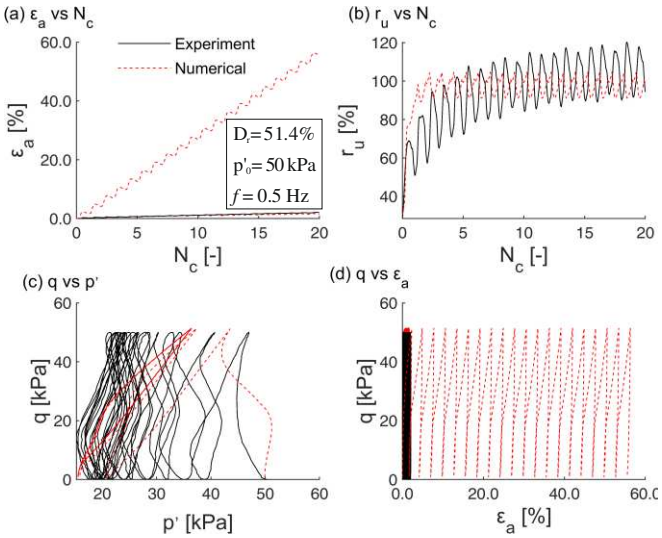

Figure 7. Undrained cyclic response: IS extension

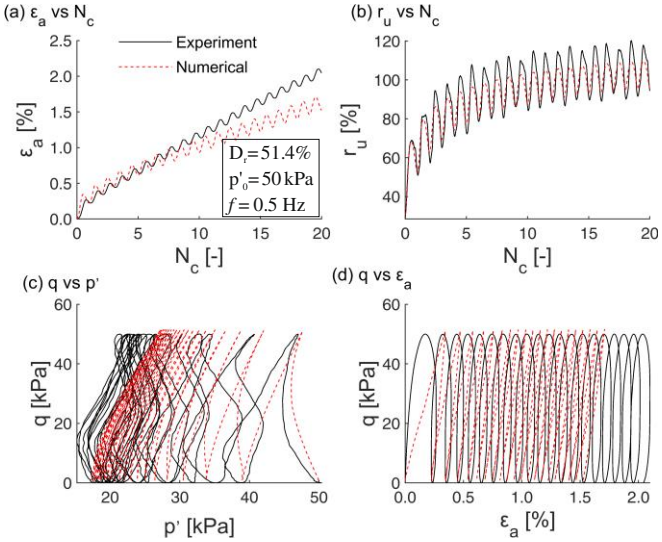

Figure 8. Undrained cyclic response: ISA extension

Figure 9 compares the response of three specimens tested at different relative density, isotropically consolidated to p'_0 = 100 kPa and loaded to a CSR = 0.75 for N_c = 20 cycles. The numerical results correspond to the simulations using the ISA extension for similar testing conditions and loading. The experimental results show higher pore water pressure accumulation (Figure 9(a))

and build-up of the cyclic axial strains (Figure 9(b)) for the relative density range considered (D_r = 21 % - D_r = 47 %) compared to the numerically computed values. Thus, in the numerical analyses the liquefaction resistance is relatively overestimated. However, the increase in liquefaction resistance with the increase of the relative density is well captured.

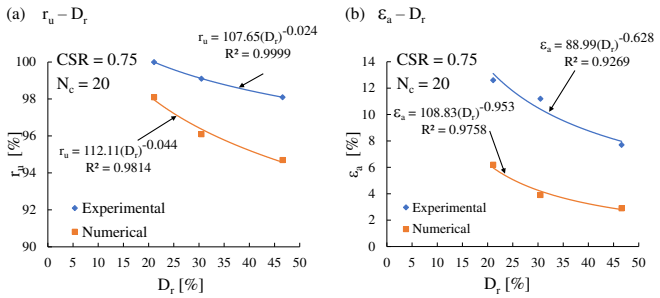

Figure 9. comparison of cyclic tests and numerical results

5 CONCLUSIONS

The capability of the hypoplastic constitutive model by von Wolffersdorff (1996), with the intergranular strain extensions by Niemunis and Herle (1997) and the modification of Wegener and Herle (2014) on the one side, and the ISA approach by Poblete et al. (2016) on the other side, has been investigated simulating monotonic and cyclic triaxial tests on a silty sand from Ethiopia.

Under undrained monotonic loading conditions, the calculated development of deviatoric stress and excess pore water pressure with increasing axial strain corresponds well to the values measured in the experiments when the HP model with the IS extension was used. The IS parameters were calibrated based on a cyclic test. However, when the same parameters were used for another test with cyclic loading, the results showed excessive strain accumulation and faster pore pressure build-up. In contrast, the use of the ISA extension appears to attenuate the excessive strain accumulation.

6 ACKNOWLEDGEMENTS

Financial support for this work was provided by the collaboration of Mekelle University under the Ministry of Science and Higher Education of Ethiopia (MoSH) and the German Academic Exchange Service (DAAD) within the EECBP Home Grown Ph.D. Scholarship Program and the University of Kassel.

7 REFERENCES

Abdelkadr, A. 2023. Cyclic behaviour and liquefaction potential of silty sand: Experimental and numerical investigations. PhD Dissertation. University of Kassel, Germany Schriftenreihe Geotechnik, Heft 29. Kassel: Kassel Univ. Press.

Abdelkadr, A., Reul, O., Ojha, L.N. 2022. Experimental study on the cyclic behaviour and liquefaction potential of typical silty sand from Tigray region in Ethiopia. Proc. 20th International Conference on Soil Mechanics and Geotechnical Engineering. Sydney, 2069–2074.

Bao, Y., Sture, S. 2011. Numerical Modeling of Cyclic Mobility based on Fuzzy-Set Concepts in Plasticity Theory. *Computers and Geotechnics* 38 (3), 375–382.

Belkhatir, M., Arab, A., Della, N., Missoum, H., Schanz, T. 2010. Liquefaction Resistance of Chlef River Silty Sand: Effect of Low Plastic Fines and other Parameters. *Acta Polytechnica Hungarica* 7 (2), 119–137.

Bonini, M., Corti, G., Innocenti, F., Manetti, P., Mazzarini, F., Abebe, T., Pecskay, Z. 2005. Evolution of the Main Ethiopian Rift in the frame of Afar and Kenya rifts propagation. *Tectonics* 24 (TC1007), 1-21.

Cudmani, R. 2013. Soil liquefaction: Mechanism and Assessment of Liquefaction Susceptibility: International Conference on Seismic Design of Industrial Facilities. RWTH Aachen University.

Ertek, M.K., Demir, G. 2017. Evaluation of liquefaction potential and post-liquefaction settlements in a coastal region in Atakum. *Arab J Geosci* 10 (232), 1–16.

Herle, I., Gudehus, G. 1999. Determination of parameters of a hypoplastic constitutive model from properties of grain assemblies. *Mechanics of Cohesive-frictional Materials* 4, 461–486.

Hleibieh, J., Herle, I. 2019. The performance of a hypoplastic constitutive model in predictions of centrifuge experiments under earthquake conditions. *Soil Dynamics and Earthquake Engineering* 122, 310–317.

Lade, P. V.; Yamamuro, J. A. (Eds.) 1999. Physics and Mechanics of Soil Liquefaction. Rotterdam, Netherlands: A.A. Balkema.

Niemunis, A., Herle, I. 1997. Hypoplastic model for cohesionless soils with elastic strain range. *Mechanics of Cohesive-frictional Materials* (2), 279–299.

Poblete, M., Fuentes, W., Triantafyllidis, T. 2016. On the simulation of multidimensional cyclic loading with intergranular strain. *Acta Geotech.* 11 (6), 1263–1285.

Tochnog Professional Company 2021. TOCHNOG PROFESSIONAL-User's manual. Available online at http://www.feat.nl, checked on 11/30/2021.

Tsuchida, H. 1970. Prediction and Countermeasure Against the Liquefaction in Sand Deposits. *Seminar in the Port and Harbor Research Institute*, 3.1-3.33.

USGS 2019. National Earthquake Information Centre. Available online at https://earthquake.usgs.gov/data/comcat/contributor/us/.

Wegener, D., Herle, I. 2014. Prediction of permanent soil deformations due to cyclic shearing with a hypoplastic constitutive model. *geotechnik* 37 (2), 113–122.

Wolffersdorff, P.A. 1996. A hypoplastic relation for granular materials with a predefined limit state surface. *Mechanics of Cohesive-frictional Materials* 1 (3), 251–271.